

**PEER REVIEW OF ENVIRON'S OZONE SOURCE
APPORTIONMENT TECHNOLOGY AND
THE CAMX AIR QUALITY MODELS**

**REVISED FINAL REPORT
STI-996203-1732-RFR**

**Prepared by:
Naresh Kumar
Frederick W. Lurmann
Sonoma Technology, Inc.
Santa Rosa, CA**

**Prepared for:
Ohio Environmental Protection Agency
Division of Air Pollution Control
Columbus, OH**

June 1997

**PEER REVIEW OF ENVIRON'S OZONE SOURCE
APPORTIONMENT TECHNOLOGY AND
THE CAMX AIR QUALITY MODEL**

**REVISED FINAL REPORT
STI-996203-1732-RFR**

**Prepared by:
Naresh Kumar
Frederick W. Lurmann
Sonoma Technology, Inc.
5510 Skylane Boulevard, Suite 101
Santa Rosa, CA 95403**

**Prepared for:
Bill Spires
Ohio Environmental Protection Agency
Division of Air Pollution Control
1600 Watermark Drive
Columbus, OH 43216-1049**

June 30, 1997

TABLE OF CONTENTS

<u>Section</u>	<u>Page</u>
LIST OF FIGURES	v
LIST OF TABLES	vii
1. INTRODUCTION	1-1
2. OZONE SOURCE APPORTIONMENT TECHNOLOGY DESCRIPTION	2-1
2.1 TIMING TRACERS	2-1
2.2 OZONE REACTION TRACERS	2-1
2.2.1 Chemical Change	2-2
3. REVIEW OF THE OZONE SOURCE APPORTIONMENT TECHNOLOGY	3-1
3.1 TECHNICAL BASIS OF THE OSAT FORMULATION	3-1
3.1.1 Timing Tracers	3-2
3.1.2 Ozone Reaction Tracers	3-2
3.1.3 Distinguishing VOC-Limited from NO _x -Limited Ozone Formation	3-3
3.1.4 Distinguishing VOC Reactivity Differences	3-11
3.1.5 Testing of the OSAT with UAM-IV in Los Angeles Simulations	3-12
3.1.6 Assignment of Source Attribution At Night	3-13
3.2 SUMMARY	3-13
4. BRIEF REVIEW OF THE CAMX AIR QUALITY MODEL	4-1
4.1 CODE STRUCTURE	4-1
4.2 CHEMISTRY	4-2
4.3 TRANSPORT AND GRID NESTING	4-5
4.4 PLUME-IN-GRID (PiG)	4-5
4.5 DEPOSITION	4-7
4.6 SUMMARY	4-7
5. REFERENCES	5-1

LIST OF FIGURES

<u>Figure</u>	<u>Page</u>
3-1. Simulated ozone concentrations and $P_{H_2O_2}/P_{HNO_3}$ ratios for the box model simulation with an initial VOC/NO _x ratio of 10 ppbC/ppb and initial NO _x concentration of 30 ppb.....	3-7
3-2. Simulated ozone concentrations and $P_{H_2O_2}/P_{HNO_3}$ ratios for the box model simulation with an initial VOC/NO _x ratio of 10 ppbC/ppb and initial NO _x concentration of 60 ppb.....	3-8
3-3. Simulated ozone concentrations and $P_{H_2O_2}/P_{HNO_3}$ ratios for the box model simulation with an initial VOC/NO _x ratio of 20 ppbC/ppb and initial NO _x concentration of 15 ppb.....	3-9
3-4. Simulated ozone concentrations and $P_{H_2O_2}/P_{HNO_3}$ ratios for the box model simulation with an initial VOC/NO _x ratio of 20 ppbC/ppb and initial NO _x concentration of 30 ppb.....	3-10
4-1. Comparison of ozone and H ₂ O ₂ concentrations calculated with the CAMx and LSODE solvers for a daytime initial value problem with an urban VOC mixture, initial VOC/NO _x = 5, and initial NO _x = 200 ppb	4-3
4-2. Comparison of ozone and H ₂ O ₂ concentrations calculated with the CAMx and LSODE solvers for a daytime initial value problem with an urban VOC mixture, initial VOC/NO _x = 20, and initial NO _x = 200 ppb	4-3
4-3. Comparison of ozone and H ₂ O ₂ concentrations calculated with the CAMx and LSODE solvers for a daytime initial value problem with an urban VOC mixture, initial VOC/NO _x = 20, and initial NO _x = 20 ppb	4-4
4-4. Comparison of ozone and H ₂ O ₂ concentrations calculated with the CAMx and LSODE solvers for a daytime initial value problem with initial isoprene/NO _x = 10, and initial NO _x = 4 ppb.....	4-4
4-5. Comparison of ozone and H ₂ O ₂ concentrations calculated with the CAMx and LSODE solvers for a nighttime initial value problem with an urban VOC mixture, initial VOC/NO _x = 5, initial ozone = 200 ppb, and initial NO = 50 ppb	4-6
4-6. Comparison of ozone and H ₂ O ₂ concentrations calculated with the CAMx and LSODE solvers for a nighttime initial value problem with initial isoprene/NO _x = 5, initial ozone = 200 ppb, and initial NO = 50 ppb.....	4-6

LIST OF TABLES

<u>Table</u>	<u>Page</u>
3-1. Change in ozone as a result of VOC or NO _x pulse at a given P _{H2O2} /P _{HNO3} ratio for initial VOC/NO _x of 10 and initial VOC of 300 ppb.....	3-5
3-2. Change in ozone as a result of VOC or NO _x pulse at a given P _{H2O2} /P _{HNO3} ratio for initial VOC/NO _x of 20 and initial VOC of 300 ppb.....	3-5
3-3. Change in ozone as a result of VOC or NO _x pulse at a given P _{H2O2} /P _{HNO3} ratio for initial VOC/NO _x of 10 and initial VOC of 600 ppb.....	3-6
3-4. Table 3-4. Change in ozone as a result of VOC or NO _x pulse at a given P _{H2O2} /P _{HNO3} ratio for initial VOC/NO _x of 20 and initial VOC of 600 ppb.....	3-6
3-5. Percent ozone formed under NO _x -or VOC- limited conditions for different values of P _{H2O2} /P _{HNO3} ratio used as cutoff point.....	3-11

1. INTRODUCTION

Photochemical air quality models are applied to estimate the effects of VOC and NO_x emission control measures on ambient ozone concentrations. Traditionally, the effects of each control strategy have been quantified in individual simulations which could be compared to baseline simulations. Each control measure required one model simulation. ENVIRON Corporation has developed new Ozone Source Apportionment Technology (OSAT) to improve the efficiency of this process. The OSAT is used in conjunction with a 3-D photochemical air quality model to estimate the contributions of emissions from multiple source regions and multiple precursor species to ozone concentrations at downwind receptors in a single model simulation. The OSAT also estimates the amount of ozone formed under locally VOC- or NO_x-limited conditions which can help in the design of effective ozone control strategies. This technology has the potential to greatly reduce the number of simulations needed for identification of effective control strategies. The OSAT has been implemented in the UAM-IV model and tested in California's South Coast Air Basin (Yarwood et al., 1996). The OSAT has also been implemented in ENVIRON's Comprehensive Air Quality Model with Extensions (CAMx) and applied in the eastern US for Ozone Transport Assessment Group (OTAG) episodes (Morris et al., 1997). The CAMx model was developed for regional-scale modeling of ozone and other pollutants (ENVIRON, 1997).

The purpose of this study is twofold. The primary purpose is to review the technical formulation of the ozone source apportionment technology that is implemented in the CAMx model. The secondary purpose is to review the CAMx air quality models and identify the principal similarities and differences between the CAMx model and UAM-V model (SAI, 1995). Both elements are designed to evaluate the methods used to simulate the relationship between ozone concentrations and emissions in OTAG simulations. The scope of the study is limited to reviewing reports on the models and performing selected quantitative evaluations of certain components of the models. The scope does not include a complete review of the source codes or independent verification of simulation model results.

2. OZONE SOURCE APPORTIONMENT TECHNOLOGY DESCRIPTION

The OSAT introduces user-defined pollutant tracers into the modeling system to estimate the source apportionment (Yarwood et al., 1996). The OSAT uses two distinct types of tracer species, “timing tracers” and “ozone reaction tracers”. The timing tracers are used to assess whether precursor emissions from a specific time period and/or source region are transported to a receptor location and, if so, the approximate transport time to reach the receptor. Timing tracers for initial and boundary concentration contributions can be employed as well. Timing tracers can be specified for arbitrarily selected time intervals and/or source groupings where a source grouping can be the emissions from (1) all sources in one geographic area, (2) specific categories of emissions in all areas, or (3) specific categories in specific areas. The ozone reaction tracers are used to track the fate of precursor emissions from each source grouping and the ozone formation attributed to those emissions. The ozone and precursor species contributions from initial and boundary concentrations can also be tracked as specific sources so that all of the contributions to ozone can be accounted for in the apportionment.

2.1 TIMING TRACERS

Pairs of timing tracers are used in the OSAT for each time interval and/or source grouping. Each pair consists of an inert tracer and a decay tracer. The inert tracer is transported and diffused, but not subjected to deposition or chemical reaction losses. The decay tracer is transported, diffused, and lost at a constant rate. The inert and decay tracers are emitted into the surface grid cells at a constant rate for the appropriate times and/or regions. After release, the concentrations of decay tracers decay exponentially due to the constant loss rate. Since both tracers are affected identically by transport and diffusion, differences in predicted concentrations between the two are due only to the first-order loss of the decay tracer. The presence of inert tracers from a given source region (A) at a receptor region (B) indicates that pollutants are transported from A to B. The average age or transport time of the material transported from region A to region B can be estimated from the difference of the inert and decay tracer concentrations. The inert and decay tracers can be released at user-specified time periods and, once introduced, the tracers are kept in the simulation until the end of the run. For example, in a typical regional simulation, distinct timing tracers may be released four times per day (at uniform 6-hour intervals) in 10 different regions and new sets of tracers may be released each day. Thus, by the end of a typical five-day simulation, there would be 400 timing tracers (2 types x 10 regions x 4 per day x 5 days) included in the simulation.

2.2 OZONE REACTION TRACERS

Four ozone-reaction tracers are used for each source grouping to account for the contributions of the emissions (or initial and boundary concentrations) to ozone formation. Separate tracers are used to track ozone formation occurring under NO_x and VOC-limited conditions. The four types of ozone-reaction tracers are:

1. N_i is a tracer for reactive NO_x from source grouping i . N_i is emitted with the same spatial and temporal distribution as NO_x emissions for source grouping i . N_i reacts at the same rate as NO_x ($d\text{NO}_x/dt$) in each grid cell.
2. V_i is a tracer for reactive VOC from source grouping i . V_i is emitted with the same spatial and temporal distribution as VOC emissions for source grouping i . V_i reacts at the same rate as VOC ($d\text{VOC}/dt$) in each grid cell.
3. $\text{O3}V_i$ is a tracer of ozone formation under VOC-limited conditions attributed to source grouping i . If ozone is determined to be VOC-limited for a given grid cell at a given time, $\text{O3}V_i$ is formed in proportion to the local rate of ozone formation ($d\text{O}_3/dt$) weighted by the distribution of VOC precursors (V_i).
4. $\text{O3}N_i$ is a tracer of ozone formation under NO_x -limited conditions attributed to source grouping i . If ozone is determined to be NO_x -limited for a given grid cell at a given time, $\text{O3}N_i$ is formed in proportion to the local rate of ozone formation ($d\text{O}_3/dt$) weighted by the distribution of NO_x precursors (N_i).

The rates of emission of the N_i and V_i tracers are set equal to the total NO_x and VOC emissions for each source grouping. For the initial condition (IC) source grouping, the tracers (N_{IC} and V_{IC}) are initialized from the initial concentration fields and receive no additional mass after the start of the simulation. For the boundary conditions (BC) source grouping, the fluxes of NO_x and VOC entering the modeling domain are effectively interpreted as emissions of the N_{BC} and V_{BC} tracers at the model boundaries. Unlike emission source groupings, boundary and initial conditions also introduce ozone directly into the model. Since there is no objective way of determining the conditions under which the initial and boundary ozone was formed, the OSAT divides it equally between the $\text{O3}N$ and $\text{O3}V$ tracers. However, subsequent ozone formation from boundary and initial VOCs and NO_x is allocated to the $\text{O3}V$ and $\text{O3}N$ tracers based on the conditions under which the ozone was formed.

The N_i , V_i , $\text{O3}N_i$, and $\text{O3}V_i$ tracers are deposited in the surface cell at rates determined by the host air quality model's deposition algorithm. The deposition velocity for NO_x is a weighted average of NO and NO_2 . Similarly, the deposition velocity for the lumped VOC tracer is a concentration weighted average of deposition velocities of the individual CB-IV organic species in the grid cell at that time step. These tracers are also transported and diffused in the same manner as other species in the host air quality model.

2.2.1 Chemical Change

The chemical change in the tracer concentrations are proportional to the change in the total concentrations. For example, the NO_x tracer (N_i) concentration in each grid cell at each time step decays according to the chemical change in the model predicted NO_x (ΔNO_x per Δt) weighted by the tracer contribution to the total NO_x tracers from all source groupings:

$$N_i = N_i + \Delta NO_x * \frac{N_i}{\sum N_i} \quad (2-1)$$

The VOC tracer (V_i) concentration in each grid cell at each time step decays according to the chemical change in the model predicted VOC (ΔVOC per Δt) weighted by the tracer contribution to the total of VOC tracers (weighted by the OH-reactivity of each V tracer) from all source groupings. The OH-reactivity of each source grouping (kOH_i) is calculated at the start of each simulation period by averaging the OH rate constants of the speciated VOC emissions for each source grouping. The following equation is used to calculate the chemical change of the V_i tracer mass:

$$V_i = V_i + \Delta VOC * \frac{V_i * kOH_i}{\sum (V_i * kOH_i)} \quad (2-2)$$

The O3N and O3V tracers for each source grouping accumulate a weighted fraction of the ozone production/destruction activity (ΔO_3 per Δt) that occurs in each grid cell at each time step. The procedures for apportioning ΔO_3 between the O3N_i and O3V_i tracers depends on whether the chemical change in ozone is positive or negative and whether the ratio of hydrogen peroxide (H_2O_2) to nitric acid (HNO_3) production rates indicate conditions are NO_x -limited or VOC-limited. The procedures are as follows:

1. If the chemical change in ozone (ΔO_3) is positive at a particular time and place and the ozone production is estimated to be NO_x -limited, which is indicated by a ratio of H_2O_2 to HNO_3 production rates exceeding 0.35, the O3N_i ozone tracer concentration is computed from:

$$O3N_i = O3N_i + \Delta O3 * \frac{N_i}{\sum N_i} \quad (2-3)$$

and the O3V_i ozone tracer concentration is left unchanged.

2. If the chemical change in ozone (ΔO_3) is positive at a particular time and place and the ozone production is estimated to be VOC-limited, which is indicated by a ratio of H_2O_2 to HNO_3 production rates below 0.35, the O3V_i ozone tracer concentration is computed from:

$$O3V_i = O3V_i + \Delta O3 * \frac{V_i * kOH_i}{\sum (V_i * kOH_i)} \quad (2-4)$$

and the O3N_i ozone tracer concentration is left unchanged.

3. If the chemical change in ozone (ΔO_3) is negative at a particular time and place (i.e., ozone is chemically destroyed by high NO or alkene concentrations), then the ozone tracer concentrations are each calculated using the equations:

$$O3N_i = O3N_i + \Delta O3 * \frac{N_i}{\sum (N_i + V_i)} \quad (2-5)$$

and

$$O3V_i = O3V_i + \Delta O3 * \frac{V_i}{\sum (N_i + V_i)} \quad (2-6)$$

These equations apportion the ozone loss in proportion to the amount of NO_x and VOC emissions from the different source groupings.

3. REVIEW OF THE OZONE SOURCE APPORTIONMENT TECHNOLOGY

The OSAT documentation (Yarwood et al., 1996; 1997) was reviewed in order to assess whether its formulation was technically sound and to identify possible limitations of the methodology and its underlying assumptions. Also, as part of the review, analyses were performed to evaluate selected aspects of the OSAT and the implementation of the algorithms was spot checked in critical areas. The main goal of this review was to assess the technical basis of the OSAT formulation and to examine the validity of the underlying assumptions. A thorough code check and software quality assurance check was beyond the scope of this study.

3.1 TECHNICAL BASIS OF THE OSAT FORMULATION

The OSAT is essentially an accounting system or bookkeeping system that has been added to a host air quality model. As described in Section 2, the OSAT is designed to provide information on source-receptor transport times and to assess source apportionment of ozone and its precursors for the regions and source groups selected by the user. The scope of the methodology is robust in that it addresses all three aspects of the source ozone apportionment problem: ozone, ozone precursor capability, and timing. The methodology appears to be computationally efficient since all of the algorithms involve simple linear apportionments of NO_x, VOC, and ozone from each source grouping, and use of the same transport and dispersion algorithms used for the regular species in the host model.

It should be noted that when the accounting system (OSAT) is added, the computation speed of the combined model may be substantially lower than the speed of the host air quality model alone (with typical OSAT inputs). Also, the methodology is memory intensive and may require 10 to 50 times more memory than the host air quality model for a typical application. These requirements are reasonable considering the additional outputs generated in a single simulation. The speed and memory requirements will depend on the number of source groupings and the number of timing tracers.

It is important to recognize that there is no mathematically unique solution to the ozone source apportionment problem. The underlying science does not provide unique tracers for ozone source contributions from a mixture of sources. The chemical kinetic rate of ozone formation and destruction depend only on the total concentrations of individual reactants in a grid cell and are independent of the origin of the species. The OSAT and other source apportionment schemes [such as the Ozone Precursor Participation Analysis Technique (OPPAT) and the Anthropogenic Precursor Culpability Analysis (APCA)] are models of apportionment. Thus, we can only assess whether a specific source apportionment scheme is consistent with the available scientific knowledge, recognizing that numerous ozone allocation schemes which give different results may be consistent with the science. Our review of the OSAT and its underlying assumptions did not reveal any assumptions that are inconsistent with the current scientific understanding of the relevant processes. That is, the OSAT apportionment model is technically sound, although its results are not unique. Specific comments on the technical features of the OSAT are provided below.

3.1.1 Timing Tracers

The timing tracers are useful for determining whether emissions are transported from source region A to receptor region B and the source-receptor transport time. The timing tracers do not reveal anything about photochemistry occurring during pollutant transport and, therefore, appear much less useful than the ozone reaction tracers. The OSAT dual tracer technique is more efficient than the classical approach of releasing inert tracers every hour to assess whether and when precursor emissions reach certain receptor areas. The latter approach can rapidly lead to an unmanageable number of tracers (as would the OSAT if new tracers had to be released every hour, which they do not). The logic for simulation of the timing tracer species is similar to the logic for dealing with other inert or linearly reacting species in the host 3-D air quality model. The simulation of timing tracer transport is subject to the same types of numerical or pseudo-dispersion errors in the advection routines as all other species in the model. The numerical errors in advection can be significant because the popular air quality models (UAM-IV, UAM-V, and CAMx) use the computationally fast and inaccurate Smolarkiewicz (1983) advection scheme. Spot checks of the implementation of the timing tracer logic (for example, the logic to determine the transport time) did not reveal any flaws. Thus, the technical formulation of the timing tracers is sound, but subject to the same limitations as other species due to advection errors.

3.1.2 Ozone Reaction Tracers

The unique aspect of the OSAT lies in the second category of tracers, the ozone-reaction tracers, which are designed to account for the contributions of emissions of a particular source grouping to ozone in specific receptor areas. The most critical tracers are the O3V and O3N tracers which account for ozone formation under VOC-limited conditions and NO_x-limited conditions, respectively. The O3V and O3N tracers are used to attribute ozone production to source grouping based on their contributions to local VOC or NO_x concentrations, respectively. Hence, the criterion used to determine whether ozone formation is occurring under locally NO_x- or VOC-limited conditions is important.

The OSAT was designed in a manner that does not interfere with or alter the host air quality model calculations, which is an important and necessary feature. The OSAT is theoretically mass consistent with the underlying air quality model since all the tracers conserve mass. However, the implementation of the OSAT in CAMx and UAM-IV employs a renormalization step to ensure the sum of the ozone reaction tracers equal the ozone concentrations. The renormalization step is needed because the advection algorithm used in the CAMx and UAM-IV models (Smolarkiewicz, 1983) is too diffusive to preserve the relationship between the ozone reaction tracers and the model ozone concentrations on a cell-to-cell basis. The renormalization step is an easy fix to the problem associated with the inaccurate Smolarkiewicz scheme; however, it is of concern because it could also mask small errors in the OSAT implementation. The documentation reviewed for this study did not include any testing with more accurate advection schemes or without renormalization. We suggest that the OSAT be tested using a more accurate horizontal advection algorithm (e.g., Bott, 1989) with and without mass renormalization to characterize the effects of this numerical filter in the OSAT implementation.

3.1.3 Distinguishing VOC-Limited from NO_x-Limited Ozone Formation

There are no species in the photochemical mechanism that precisely indicate whether ozone formation is NO_x or VOC limited. Sillman (1995) examined the usefulness of NO_y, H₂O₂, and HNO₃ as indicators for ozone-NO_x-hydrocarbon sensitivity in urban areas. Sillman classified VOC- or NO_x-limited behavior based on the response of the peak ozone to reductions in VOC or NO_x availability. The division of ozone formation into NO_x-limited and VOC-limited regimes is linked to the abundance of the OH radical and other odd hydrogen (HO_x) species (Sillman, 1995). Odd hydrogen in polluted environments is most conveniently viewed as the sum of OH, HO₂, and RO₂ radicals (Kleinman, 1991). Ozone is formed when NO is converted to NO₂ by HO₂ or RO₂ rather than by the fast reaction of NO with ozone, as shown below:



These reactions are radical propagating or radical conserving. The production and destruction of these radical species in other reactions largely determines how long ozone formation can proceed. The important reactions for destruction of the odd hydrogen species are:



When formation of nitric acid (Equation 3-5) is the major sink for odd hydrogen, OH concentrations decrease with increasing NO_x levels and the source of radical formation is limited by availability of VOC. This condition is indicative of VOC-limited ozone production. Alternatively, when Equations 3-3 and 3-4 represent the major sink for odd hydrogen, OH formation is limited by the availability of NO to react with RO₂ and HO₂. Under the latter conditions, the rate of ozone production increases with increasing NO_x but is insensitive to VOC, as increases in VOC results in decrease of OH radical. Using this simplified chemistry, Sillman (1995) found that the ratio of the radical sink reaction product species concentrations, such as the ratio of H₂O₂ + ROOH to HNO₃, at the time of peak ozone were reliable indicators for sensitivity of peak ozone to VOC and NO_x controls.

There was a need in the OSAT to specify whether instantaneous ozone formation (at all hours of the day) was VOC or NO_x limited. Using the same rationale as Sillman (1995), the developers of the OSAT selected the ratio of the instantaneous production rates of H₂O₂ and HNO₃ (P_{H₂O₂}/P_{HNO₃}) as the indicator of the instantaneous state of ozone formation with regard to VOC or NO_x limitation. A value of 0.35 for P_{H₂O₂}/P_{HNO₃} was selected as the transition threshold between VOC-limited and NO_x-limited conditions. Ozone formation was designated as VOC limited when this ratio was less than 0.35. The threshold for OSAT was approximately consistent with the value of 0.5 for [H₂O₂ + ROOH]/[HNO₃] suggested by Sillman (1995).

There are a number of differences between Sillman's work and the OSAT application. First, Sillman used the indicator to determine whether the peak ozone was more sensitive to VOC or NO_x controls, which is not exactly the same as whether the instantaneous ozone was formed under VOC- or NO_x-limited conditions. Second, Sillman derived the numerical values for his indicator from the ratio of H₂O₂ to HNO₃ concentrations at the time of peak ozone, which are integrated values over the course of the day, rather than the instantaneous production rates (P_{H₂O₂}/P_{HNO₃}). Our concern here is not with the choice of indicator, but rather the numerical value of the threshold transition. Current understanding of atmospheric chemistry suggests that the P_{H₂O₂}/P_{HNO₃} ratio should be a reliable indicator for determining transition between the VOC- and NO_x- limited ozone production (even though P_{H₂O₂ + ROOH} might be more robust than P_{H₂O₂} alone). We felt the transition threshold for the P_{H₂O₂}/P_{HNO₃} ratio needed to be evaluated and perhaps refined.

We performed a suite of photochemical box model simulations to determine the cutoff value of P_{H₂O₂}/P_{HNO₃}, which may be used as a transition point between VOC- and NO_x- limited conditions for ozone formation. Four different tests were performed using different initial VOC/NO_x ratios and initial VOC concentrations. A version of the CB-IV chemical mechanism, which was identical to the CAMx model (i.e., with the updated isoprene chemistry), was used for the simulations. The LSODE solver was used for the solution of the chemistry using a time step of 6 minutes. The simulations were run for 18 hours, starting at 6 a.m., and the diurnal solar radiation inputs represented clear sky summer conditions in Los Angeles. The initial ozone concentration was assumed to be 10 ppb in all the simulations. There was no dilution and 5 percent of the initial VOCs and NO_x were added each hour as emissions. A pulse of NO_x or VOC (equal to 1 percent of initial concentration) was introduced at different values of P_{H₂O₂}/P_{HNO₃} and the change in ozone concentration resulting from the pulse was calculated after 6 minutes, ½ hour, and 1 hour from the start of the pulse (by comparison to a comparable simulation without the pulse). **Tables 3-1 through 3-4** show the results from the four box model simulations. In theory, the ozone concentration after the first time step (i.e., 6 minutes) should determine whether the instantaneous ozone produced is under NO_x-limited or VOC-limited conditions. However, the magnitude of the NO_x pulse used in the simulations was sufficiently large that it always inhibited ozone production in the first 6 minutes (see Tables 3-1 through 3-4). Hence, we chose to analyze the impact of the NO_x or VOC pulse on ozone after ½ or 1 hour when the inhibition effect of NO_x had dissipated. We defined the P_{H₂O₂}/P_{HNO₃} transition threshold from VOC limited to NO_x conditions as the lowest value of P_{H₂O₂}/P_{HNO₃} for which a NO_x pulse caused greater impact on ozone than a VOC pulse.

Table 3-1. Change in ozone as a result of VOC or NO_x pulse at a given P_{H2O2}/P_{HNO3} ratio for initial VOC/NO_x of 10 and initial VOC of 300 ppb.

P _{H2O2} /P _{HNO3} Ratio	Percent Change in Ozone Due to an VOC Pulse			Percent Change in Ozone Due to a NO _x Pulse		
	After 6 min	After ½ hour	After 1 hour	After 6 min	After ½ hour	After 1 hour
0.01	0.04	0.17	0.27	-0.21	-0.25	-0.26
0.03	0.03	0.12	0.16	-0.17	-0.15	-0.06
0.05	0.03	0.11	0.14	-0.15	-0.11	0.01
0.07	0.02	0.09	0.11	-0.14	-0.06	0.09
0.08	0.02	0.08	0.10	-0.13	-0.04	0.12
0.1	0.02	0.08	0.09	-0.12	-0.01	0.15
0.2	0.01	0.05	0.06	-0.09	0.06	0.23
0.3	0.01	0.05	0.05	-0.07	0.10	0.27
0.4	0.02	0.04	0.05	-0.06	0.13	0.29

Table 3-2. Change in ozone as a result of VOC or NO_x pulse at a given P_{H2O2}/P_{HNO3} ratio for initial VOC/NO_x of 20 and initial VOC of 300 ppb.

P _{H2O2} /P _{HNO3} Ratio	Percent Change in Ozone Due to an VOC Pulse			Percent Change in Ozone Due to a NO _x Pulse		
	After 6 min	After ½ hour	After 1 hour	After 6 min	After ½ hour	After 1 hour
0.01	0.06	0.25	0.37	-0.20	-0.22	-0.19
0.03	0.04	0.18	0.23	-0.14	-0.11	0.00
0.05	0.03	0.15	0.18	-0.12	-0.06	0.09
0.06	0.04	0.14	0.16	-0.11	-0.03	0.13
0.07	0.04	0.13	0.15	-0.10	0.00	0.17
0.1	0.03	0.11	0.13	-0.09	0.01	0.20
0.18	0.03	0.09	0.10	-0.05	0.08	0.27
0.19	0.02	0.08	0.09	-0.05	0.11	0.29
0.3	0.02	0.06	0.07	-0.06	0.15	0.33
0.4	0.03	0.06	0.06	-0.02	0.18	0.38

Table 3-3. Change in ozone as a result of VOC or NO_x pulse at a given P_{H2O2} /P_{HNO3} ratio for initial VOC/NO_x of 10 and initial VOC of 600 ppb.

P _{H2O2} /P _{HNO3} Ratio	Percent Change in Ozone Due to an VOC Pulse			Percent Change in Ozone Due to a NO _x Pulse		
	After 6 min	After ½ hour	After 1 hour	After 6 min	After ½ hour	After 1 hour
0.01	0.04	0.18	0.28	-0.27	-0.30	-0.28
0.03	0.03	0.14	0.18	-0.22	-0.19	-0.08
0.05	0.03	0.12	0.14	-0.20	-0.12	0.04
0.07	0.03	0.11	0.12	-0.18	-0.09	0.09
0.08	0.03	0.09	0.11	-0.17	-0.07	0.12
0.1	0.02	0.08	0.09	-0.16	-0.03	0.16
0.2	0.02	0.06	0.06	-0.13	0.05	0.25
0.21	0.02	0.05	0.05	-0.11	0.07	0.28
0.3	0.01	0.05	0.05	-0.11	0.10	0.29
0.4	0.01	0.04	0.04	-0.09	0.14	0.33

Table 3-4. Change in ozone as a result of VOC or NO_x pulse at a given P_{H2O2} /P_{HNO3} ratio for initial VOC/NO_x of 20 and initial VOC of 600 ppb.

P _{H2O2} /P _{HNO3} Ratio	Percent Change in Ozone Due to an VOC Pulse			Percent Change in Ozone Due to a NO _x Pulse		
	After 6 min	After ½ hour	After 1 hour	After 6 min	After ½ hour	After 1 hour
0.01	0.07	0.27	0.38	-0.26	-0.26	-0.18
0.03	0.05	0.20	0.23	-0.18	-0.13	0.07
0.05	0.04	0.16	0.17	-0.16	-0.04	0.17
0.06	0.04	0.14	0.15	-0.14	-0.01	0.21
0.1	0.05	0.12	0.11	-0.10	0.07	0.29
0.16	0.03	0.09	0.09	-0.11	0.09	0.32
0.17	0.03	0.08	0.08	-0.05	0.13	0.35
0.3	0.02	0.06	0.06	-0.07	0.20	0.40
0.4	0.01	0.05	0.05	-0.07	0.20	0.42

The results shown in Tables 3-1 through 3-4 indicate the threshold varies somewhat with the initial conditions and the time horizon (½ hour or 1 hour). The variability due to different initial conditions is small (which is reassuring because the method should be independent of the absolute levels of precursors). Examination of the impact of the pulse on ozone after ½ hour show threshold values of 0.2, 0.19, 0.21, and 0.17 for P_{H2O2}/P_{HNO3} for the four different simulations. Examination of the impact on ozone after 1 hour shows cutoff values of 0.08, 0.07, 0.08, and 0.05 for the four different simulations. The evolution of ozone and P_{H2O2}/P_{HNO3} ratio is shown in **Figures 3-1 through 3-4**. These figures show that the

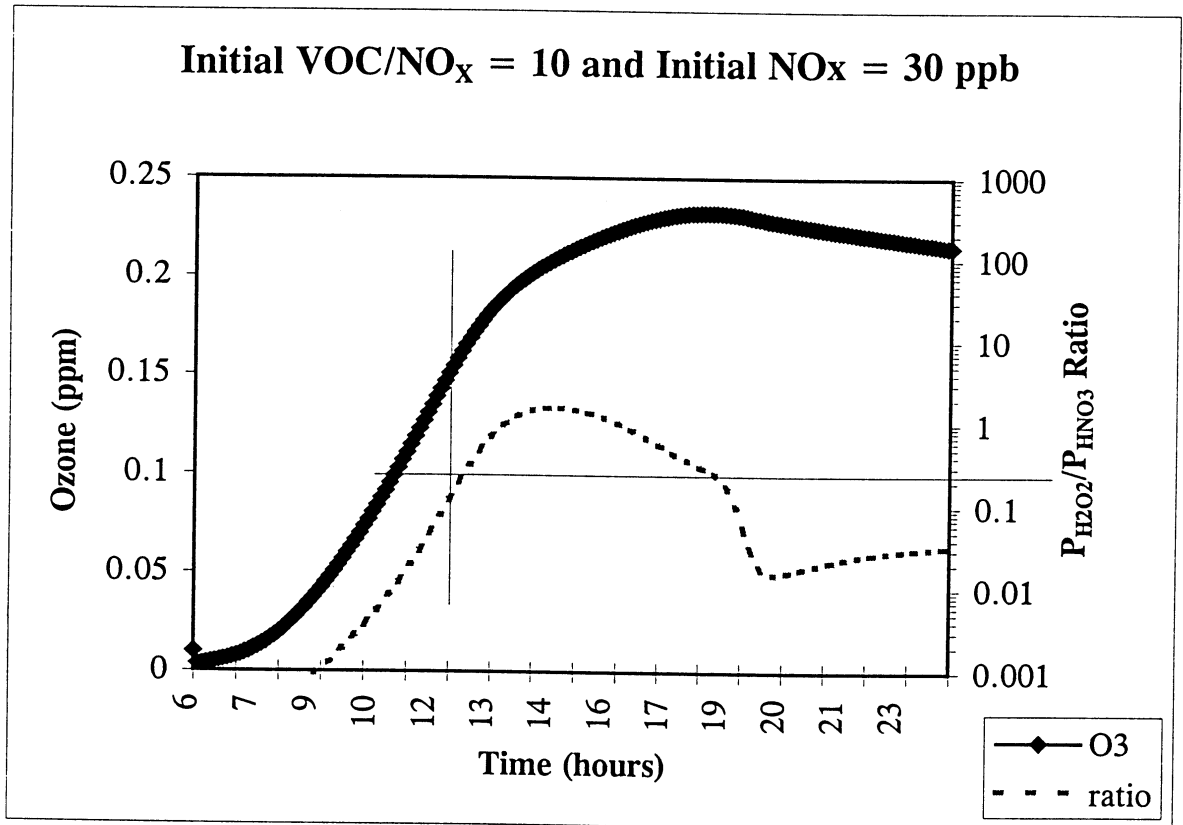


Figure 3-1. Simulated ozone concentrations and $P_{H_2O_2}/P_{HNO_3}$ ratios for the box model simulation with an initial VOC/NO_x ratio of 10 ppbC/ppb and initial NO_x concentration of 30 ppb.

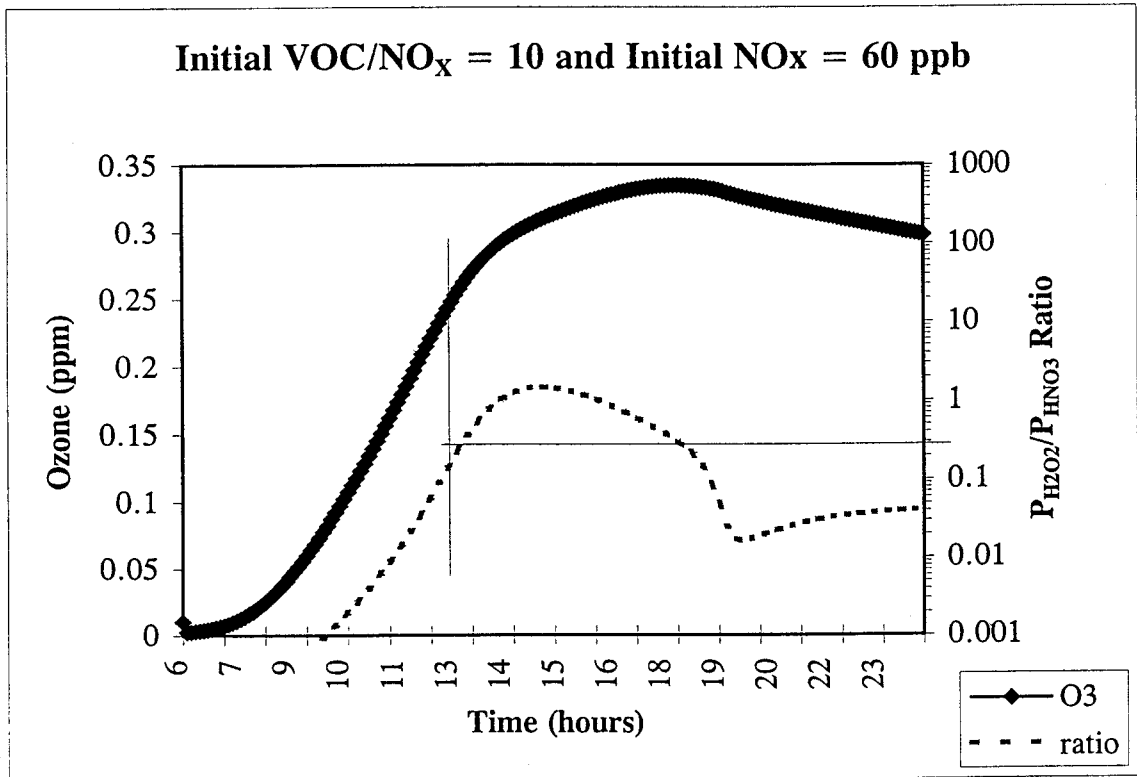


Figure 3-2. Simulated ozone concentrations and $P_{H_2O_2}/P_{HNO_3}$ ratios for the box model simulation with an initial VOC/NO_x ratio of 10 ppbC/ppb and initial NO_x concentration of 60 ppb.

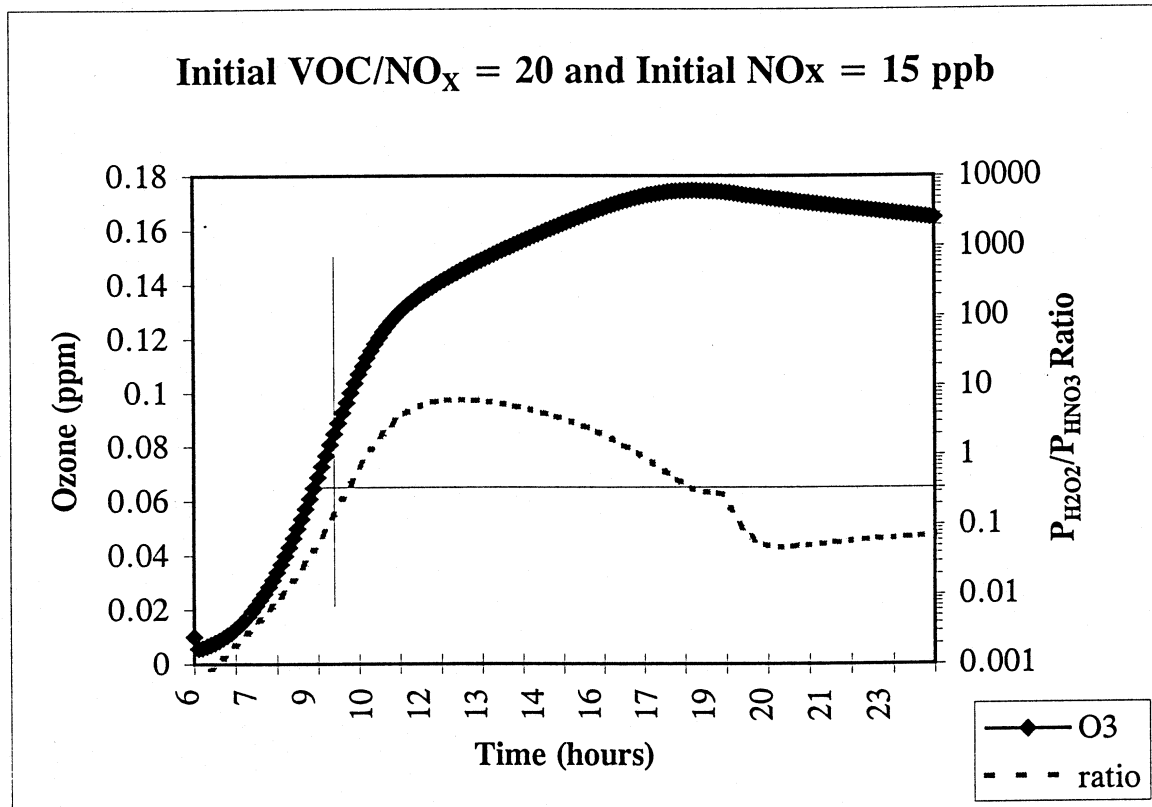


Figure 3-3. Simulated ozone concentrations and P_{H₂O₂}/P_{HNO₃} ratios for the box model simulation with an initial VOC/NO_x ratio of 20 ppbC/ppb and initial NO_x concentration of 15 ppb.

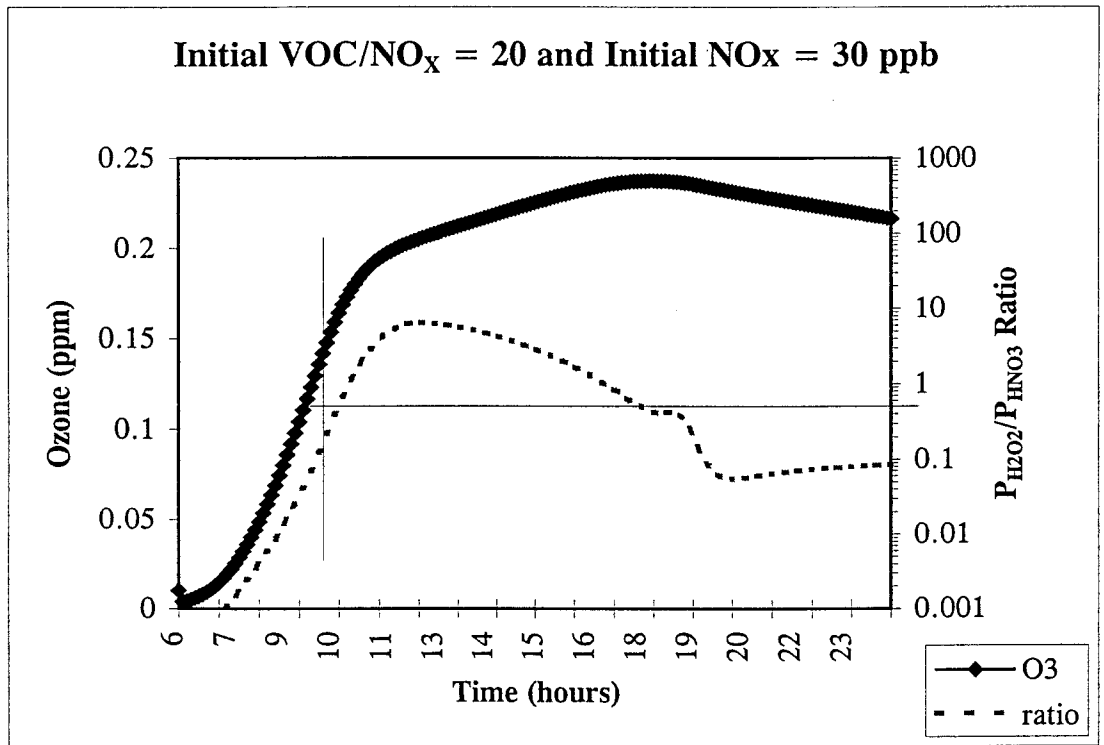


Figure 3-4. Simulated ozone concentrations and $P_{H_2O_2}/P_{HNO_3}$ ratios for the box model simulation with an initial VOC/NO_x ratio of 20 ppbC/ppb and initial NO_x concentration of 30 ppb.

$P_{\text{H}_2\text{O}_2}/P_{\text{HNO}_3}$ ratio changes so rapidly as the system runs out of NO_x that a precise specification of the ratio is probably unnecessary. That is, any threshold value between 0.05 and 0.2 may produce comparable results. Based on these results, we recommend using lower $P_{\text{H}_2\text{O}_2}/P_{\text{HNO}_3}$ threshold values (0.05 to 0.20) than the value of 0.35 currently used in the OSAT.

To examine the potential impact of using different $P_{\text{H}_2\text{O}_2}/P_{\text{HNO}_3}$ threshold values, a suite of box model simulations were performed where initial NO_x and initial VOC were randomly varied. There were a total of 2000 simulations performed. The initial NO_x varied from 10 to 200 ppb and the initial VOC varied from 0.1 to 2 ppmC, to represent mostly polluted urban conditions. The temperature varied from 273 K to 313 K and the relative humidity varied from 0.1 to 0.9. Other conditions were the same as in the other box model simulations described earlier except that there were no emissions. The means of initial VOC and initial NO_x used in all the simulations were 1.06 ppm and 106 ppb, respectively. The means of temperature and relative humidities for all the simulations were 293.3 K and 0.51, respectively. **Table 3-5** shows the attribution of ozone produced under NO_x -limited and VOC-limited conditions for different values of $P_{\text{H}_2\text{O}_2}/P_{\text{HNO}_3}$ cutoff used. Ozone destruction rates were not added in these calculations. The magnitude of the differences for this hypothetical group of runs was as follows: the average amount of ozone formed under NO_x -limited conditions was 25, 15, and 12 percent with threshold ratios of 0.05, 0.20, and 0.35, respectively. Thus, at least for the hypothetical cases, there were noticeable differences for the ozone source attribution with values of $P_{\text{H}_2\text{O}_2}/P_{\text{HNO}_3}$ ranging from 0.05 to 0.35. To better understand the sensitivity of ozone attribution to the threshold, full regional simulations with the OSAT are recommended.

Table 3-5. Percent ozone formed under NO_x - or VOC-limited conditions for different values of $P_{\text{H}_2\text{O}_2}/P_{\text{HNO}_3}$ ratio used as cutoff point.

$P_{\text{H}_2\text{O}_2}/P_{\text{HNO}_3}$ Ratio Cutoff	Percent Ozone Formed Under NO_x -Limited Conditions	Percent Ozone Formed Under VOC-Limited Conditions
0.05	25.5	74.5
0.2	15.0	85.0
0.35	11.7	88.3

3.1.4 Distinguishing VOC Reactivity Differences

The OSAT methodology attributes ozone to VOC emissions as a lumped species for different source groupings. Depending on how the source groupings are defined, this may not distinguish VOC reactivity differences well. The weighting of VOC emissions by OH rate constant alone is an approximate mean to distinguish their reactivity differences and no accounting is made for the differences in the reactivity of the product species from different VOC or of the reactions of alkenes with ozone or the NO_3 radical at night. To fully distinguish VOC reactivity differences, each CB-IV VOC species which is emitted would need to be treated as a separate emission category, which would greatly increase the number of source groupings, and require an unusually large number of tracers. This feature should be recognized as one of the

simplifying assumptions incorporated into the OSAT. Provided that biogenic VOC emissions are treated as a separate source grouping, the present treatment of reactivity in the OSAT is probably adequate for its intended use.

3.1.5 Testing of the OSAT with UAM-IV in Los Angeles Simulations

It should be recognized that the OSAT predicted source attribution is valid only for the conditions of the simulation and, since the photochemical system is nonlinear, significant deviations from those conditions will perturb the system and change the source attribution. That is, OSAT will not provide accurate source attribution for large emission changes (it was never intended to), however, when applied in a stepwise manner, it may point to effective strategies. It is important to evaluate how well it works and over what range its source attributions should be considered reliable.

All nonlinear systems behave linearly for small enough changes in inputs. Even though the photochemical system is nonlinear, the OSAT source attribution should be valid for infinitesimally small emission changes and one should be able to test the accuracy of OSAT for such changes. In fact, such testing is necessary to establish the scientific credibility of the method. The obvious method of testing the OSAT is to introduce a small pulse (i.e., an infinitesimal change in NO_x or VOC emissions) at a source grouping and analyze the response at a receptor to check whether it matches what is predicted by the OSAT methodology.

The OSAT development report indicated that, because of the numerical noise in the UAM-IV, the smallest regionally targeted emissions change for which the OSAT was evaluated was a 20 percent reduction in NO_x in one of 17 regions in the South Coast Air Basin (Yarwood et al., 1996). Actually, 10 different simulations with VOC or NO_x emissions reduced by 20 percent were performed to evaluate the OSAT. The 20 percent emissions change in these regions is greater than an infinitesimal change and may be expected to cause some deviation from linearity in the response. The results were evaluated at the peak ozone receptor and integrated over a wider area. The integrated ozone response is probably more meaningful than the maximum ozone receptor response for the intended use of the OSAT (i.e., identifying the relative contributions of source regions categories to elevated ozone concentrations). The integrated ozone response compared more favorably with the expected results than those for the maximum ozone response at the peak receptor. The ratio of the UAM-IV results to the OSAT results for integrated ozone response varied between 0.08 and 0.33 for the case where the expected ratio of 0.20. For 7 of the 10 cases, the ratio of UAM-IV results to OSAT results were within ± 20 percent of the expected ratio (0.20), which is reasonably good. For the maximum ozone response, the ratio of the UAM-IV results to the OSAT results varied between 0.07 and 0.96, and were usually biased high compared to the expected ratio of 0.20. The evaluation results for the integrated ozone response did not show any pattern of systematic bias and were encouraging because the “factor of two accuracy” is probably sufficient for the intended purpose of the OSAT. However, the OSAT failed the test for the maximum ozone response at the peak receptor in the Los Angeles simulations. Yarwood et al. (1996) ascribed the large errors and positive bias to the “idiosyncrasies of the Smolarkiewicz advection solver.” We agree that these tests of

OSAT were severely compromised by the limitations of the Smolarkiewicz scheme. The results of the Los Angeles simulations should not be interpreted as validation of the method or grounds for rejection of the method because they are flawed. We recommend testing the OSAT with a more accurate advection scheme and with smaller emission changes in order to test the source attribution adequately. The current evaluation is inadequate and inconclusive.

3.1.6 Assignment of Source Attribution At Night

As described in Section 2, when ozone is chemically destroyed at night (or any time when there is a net loss in the chemistry operator), the $O3N_i$ and $O3V_i$ tracers in the OSAT are both assumed to be affected proportionally. This assumption has no fundamental basis and can introduce uncertainty in the OSAT predictions. Ozone can be chemically destroyed by NO, NO₂, and/or alkenes and the OSAT does not attempt to assign the loss to the precursor species responsible for the loss. While it is important to keep track of the O₃ destruction for mass consistency, dividing the ozone loss term between the $O3N_i$ and $O3V_i$ tracers in proportion to N_i and V_i should be recognized as an arbitrary assumption. It would be beneficial to quantify (or bound) the uncertainties associated with the assumption and assess whether the assumption is likely to introduce bias into the OSAT results.

The present scheme may be an efficient, but approximate method of assigning the ozone loss. Most other schemes for tracking this effect more carefully would involve additional tracer species, such as ozone tracers for losses due to NO_x and alkene scavenging, which would add to the memory and computational burden of the OSAT. Limited testing of more detailed schemes may be warranted to assess whether there are benefits from refinements in this area.

3.2 SUMMARY

Our review of the OSAT and its underlying assumptions did not reveal any assumptions that are inconsistent with the current scientific understanding of the relevant processes. The OSAT apportionment model is technically sound, although its results are approximate and are not unique. The key points from the review are as follows.

- The technical formulation of the timing tracers is sound and efficient. They appear to be less useful than the ozone reaction tracers. The accuracy of timing tracers will be limited by the accuracy of the numerical advection algorithm used in the host air quality model.
- We recommend using a lower value of the P_{H2O2}/P_{HNO3} threshold to distinguish the regimes where ozone formation is limited by NO_x versus VOCs. Our analysis suggests values between 0.05 and 0.20 are more appropriate than the value of 0.35 currently used in the OSAT.
- The OSAT methodology attributes ozone to VOC emissions as a lumped species for different source groupings, rather than distinguishing the reactivity differences of the

CB-IV VOC species. Depending on how the source groupings are defined, this may not distinguish VOC reactivity differences well. However, provided that biogenic VOC emissions are treated as a separate source grouping, the present treatment of reactivity in the OSAT is probably adequate for its intended use.

- The OSAT evaluation, which was performed using UAM-IV in Los Angeles simulations, was inadequate and inconclusive because of the limitation of the Smolarkiewicz advection solver. We recommend testing the OSAT with a more accurate advection scheme and with smaller emission changes in order to evaluate the source attribution scheme adequately.
- The source attribution of ozone when it is chemical destroyed, rather than formed, is arbitrary and not based on the species responsible for the destruction. It would be beneficial to quantify (or bound) the uncertainties associated with the assumption and assess whether the assumption is likely to introduce bias into the OSAT results.
- Lastly, it is important to recognize the limitations and approximate nature of the OSAT source attribution estimates. There are no unique solutions for ozone source apportionment and the estimated apportionment are only designed to indicate how ozone would respond to small changes in emissions used for the specific simulations.

4. BRIEF REVIEW OF THE CAMX AIR QUALITY MODEL

The purpose of this element of the review is to examine the CAMx air quality model and identify the similarities and differences between the CAMx and UAM-V models. It is important to recognize at the outset that the basic formulation of the models are quite similar and that the differences are likely to be subtle, rather than large. The major similarities are that they:

- Solve the same governing equations with comparable operator splitting techniques
- Use the Carbon Bond Mechanism (CB-IV) for chemistry with fast solvers
- Have variable grid resolution
- Use the Smolarkiewicz advection scheme for transport
- Incorporate plume in grid (PiG) treatment of major point source emissions
- Use a version of Wesely (1989) dry deposition algorithm.

The scope of this review was limited in that the models were not independently applied, nor were full code evaluations conducted. The effort was focused on identifying the main differences between the two codes which could result in differences in model predictions as was seen for two OTAG episodes in the eastern United States (Kumar and Lurmann, 1997).

4.1 CODE STRUCTURE

Even though the basic formulation of the major modules is the same in both the CAMx and UAM-V models, the structure of the two computer codes are quite different. CAMx code is written in a modular style using a standard coding practice throughout the code. The array structure and memory management are designed more efficiently in CAMx, as one would expect in a new code. The CAMx code includes extensive internal documentation (comments) which makes it easy to follow the code. The internal documentation of the CAMx code is well placed and up-to-date. The UAM-V code is also modular, but it is not internally documented as well as the CAMx code. The UAM-V code is not as “clean” as the CAMx code, as it shows evidence of periodic updates and revisions over the last seven years. The differences in the code structure are to be expected given that the CAMx code was written in the 1995-1997 time frame and the UAM-V model was assembled in the early 1990s from the UAM-IV and RTM codes, which were written in the 1970s and 1980s.

Another difference in code structure is that the UAM-V uses different subroutines to simulate the same physical processes for fine grids and coarse grids, whereas the CAMx model has single subroutines for performing similar functions for fine and coarse grids, which is a better coding practice. The reason for this is probably that the UAM-V model was developed from a single-scale model, whereas the CAMx model was designed from inception as a multiscale model. The different UAM-V subroutines for fine and coarse grids include:

- Subroutine for averaging the concentrations
- Subroutine for calculating the horizontal diffusion coefficients
- Subroutine for injecting emissions into the grid
- Subroutine for plume growth
- Subroutine for injecting mass from puffs carried by the PIG submodel
- Subroutine for determining photolysis rate constant factors
- Chemistry driver
- Main subroutine for dry deposition
- Main subroutine for wet deposition
- Subroutine for performing advection in X-direction
- Subroutine for performing advection in Y-direction

There is nothing wrong with using different subroutines to perform similar functions provided that they simulate the physical processes in a consistent manner. It should not affect the calculated concentrations or the model speed in a significant way. However, it is a rather awkward design because there are large amounts of duplicate code in the UAM-V model.

4.2 CHEMISTRY

Both models use the CBM-IV chemical mechanism with updated isoprene reactions. The models use different numerical methods to solve the chemical kinetic rate equations. Both models employ fast numerical solvers for chemistry. The CAMx chemistry solver uses a hybrid numerical scheme to solve the gas-phase chemistry. The fast-reacting species are solved using a second order implicit Runge-Kutta method, the slow-reacting species are solved explicitly, and the radicals are solved using the steady-state approximation. The UAM-V chemistry solver also uses steady-state approximation for the radical species, but uses Newton-Raphson algorithm for the remainder of the species. Both solvers use various approximations to speed up the solution at night. The use of different chemistry solvers in the two models may account for the difference in results from the two models.

The CAMx solver was compared to the LSODE solver, which is a highly accurate Gear solver, for several scenarios using a photochemical box model. **Figures 4-1 through 4-3** show comparisons of ozone and H₂O₂ concentrations calculated with the CAMx and LSODE solvers for a daytime initial value problem with an urban VOC mixture, initial VOC/NO_x ratios of 5 and 20 ppbC/ppb, and initial NO_x concentrations of 20 and 200 ppb. The result for the low VOC/NO_x ratio case (Figure 4-1) compare extremely well for ozone throughout the simulation and for H₂O₂ in the daytime. The CAMX solver underestimated the H₂O₂ concentrations at night in this case. The results for the two cases with higher initial VOC to NO_x ratios (Figures 4-2 and 4-3) show good agreement for ozone and H₂O₂ throughout the simulations. **Figure 4-4** shows the results for a daytime isoprene - NO_x mixture with an initial isoprene/NO_x ratio of 10 ppbC/ppb and an initial NO_x concentration of 4 ppb. The results for this isoprene/NO_x case show the CAMx solver predictions compare extremely well for both ozone and H₂O₂ throughout the simulation.

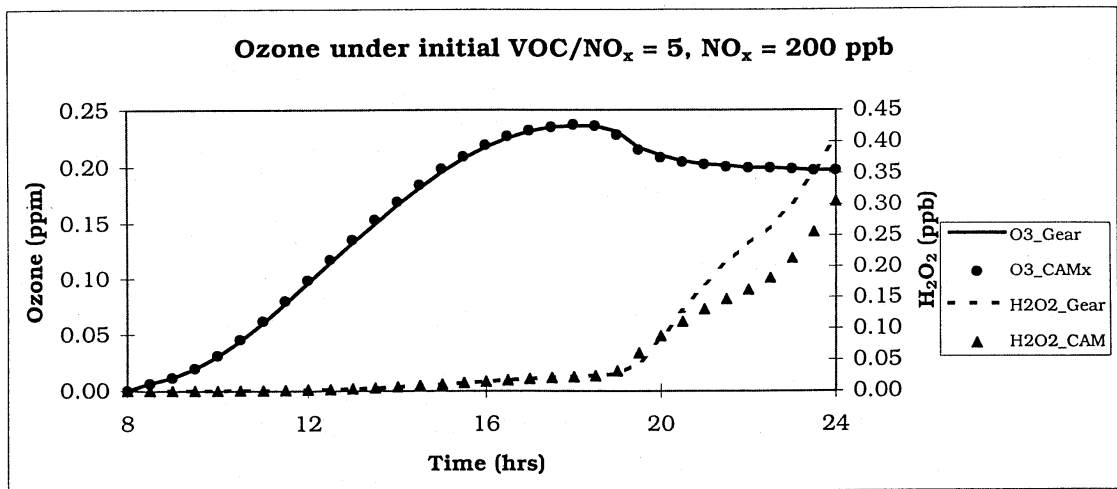


Figure 4-1. Comparison of ozone and H₂O₂ concentrations calculated with the CAMx and LSODE solvers for a daytime initial value problem with an urban VOC mixture, initial VOC/NO_x = 5, and initial NO_x = 200 ppb

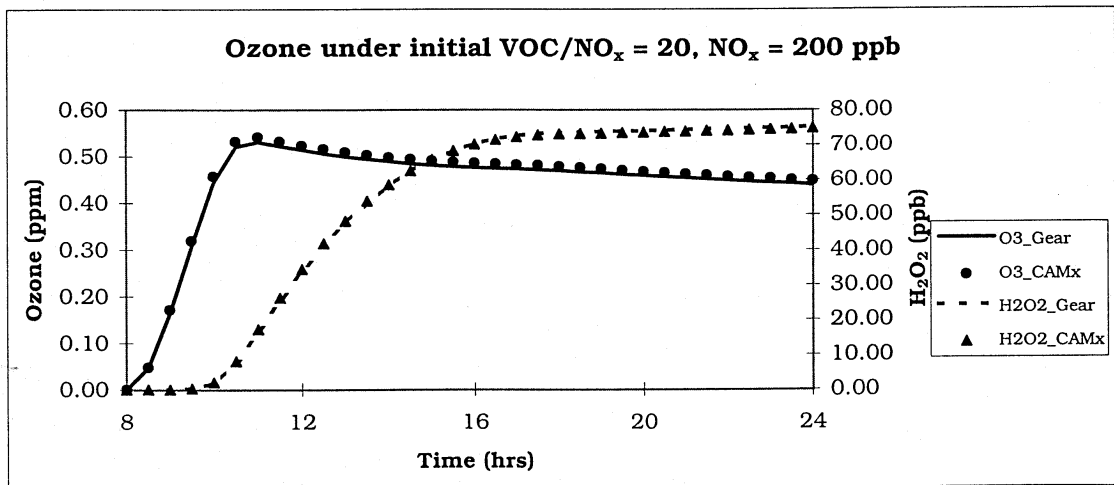


Figure 4-2. Comparison of ozone and H₂O₂ concentrations calculated with the CAMx and LSODE solvers for a daytime initial value problem with an urban VOC mixture, initial VOC/NO_x = 20, and initial NO_x = 200 ppb

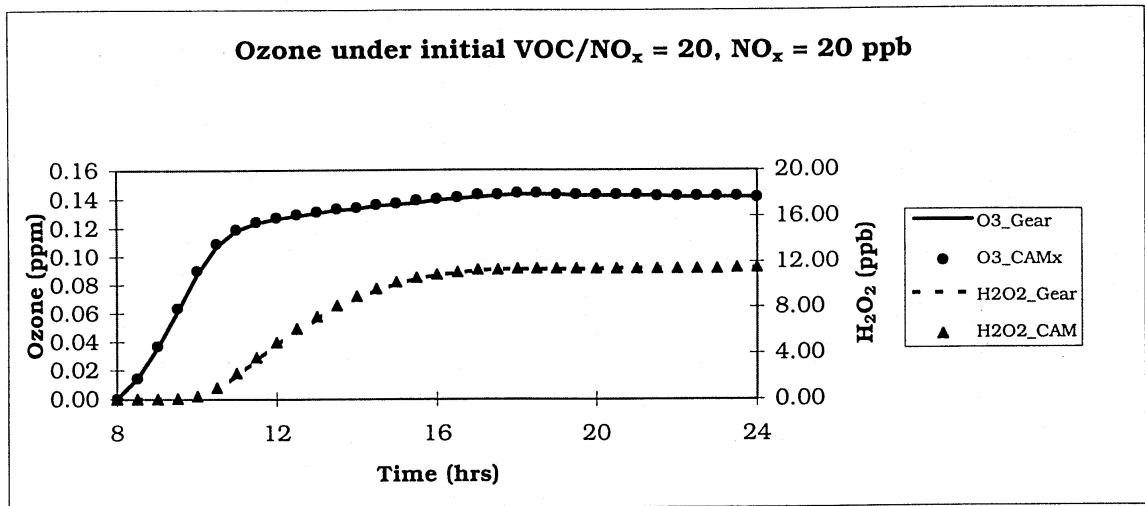


Figure 4-3. Comparison of ozone and H₂O₂ concentrations calculated with the CAMx and LSODE solvers for a daytime initial value problem with an urban VOC mixture, initial VOC/NO_x = 20, and initial NO_x = 20 ppb

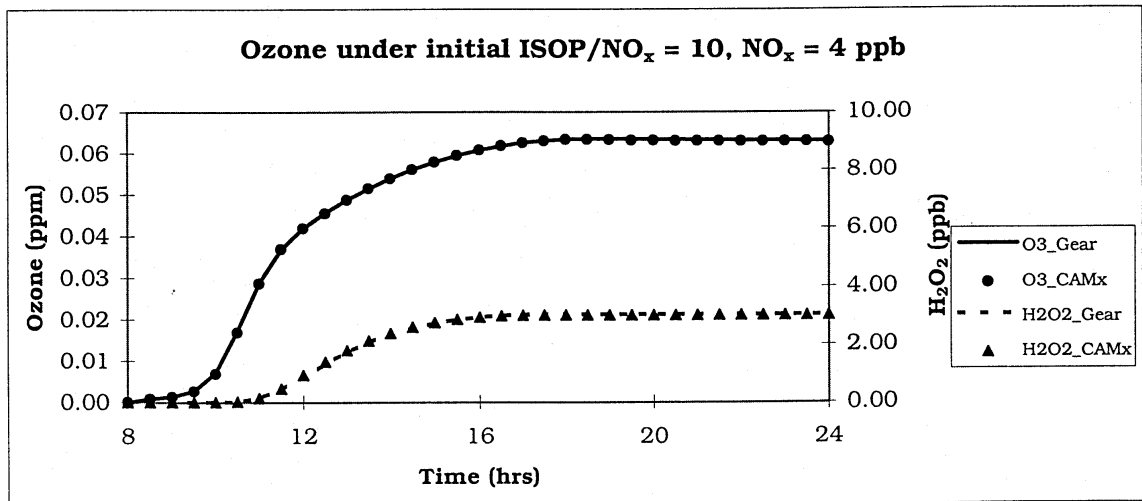


Figure 4-4. Comparison of ozone and H₂O₂ concentrations calculated with the CAMx and LSODE solvers for a daytime initial value problem with initial isoprene/NO_x = 10, and initial NO_x = 4 ppb

The results for two nighttime cases are shown in **Figures 4-5 and 4-6**. These cases were initialized with 200 ppb of ozone, 50 ppb of NO, and either 250 ppbC of urban VOC or isoprene. The CAMx and LSODE solvers give very similar predictions for ozone and for these nighttime cases. All of these cases are numerically stiff and have exaggerated conditions relative to those that the solver would normally encounter. All of the results are considered accurate (i.e., within ± 15 percent) for a fast solver. Most of the results are comparable to those shown in the CAMx development report (ENVIRON, 1997).

No attempt was made to carry out comparable evaluation of the UAM-V solver because its license restricts extracting and testing components of the modeling system. There is a need to compare the two chemistry solvers against LSODE solutions in a stand-alone box model simulation to characterize the conditions where they agree and diverge. Our review of the two solvers suggests they probably have comparable accuracy during the daytime and the CAMx solver probably has better accuracy than the UAM-V solver at night. The CAMx solver has the added advantage of conserving nitrogen mass. The UAM-V chemistry solver does not conserve nitrogen and it employs an unphysical renormalization of nitrogen species after each step.

4.3 TRANSPORT AND GRID NESTING

The CAMx and the UAM-V models both employ the Smolarkiewicz advection scheme for horizontal transport and, therefore, should produce nearly identical results for solution of the horizontal transport equation. Numerous reviews of numerical methods (e.g., Chock 1991; Dabdub and Seinfeld, 1994; Odman et al., 1996) show there are more accurate methods for simulating horizontal advection than Smolarkiewicz scheme, so it is not clear why these two models are using this outdated method.

Both models solve for horizontal diffusion using explicit methods. The two models also use a similar numerical approach for solving the vertical transport equations (advection and diffusion) and, except for coding differences, should obtain similar results.

The procedures used for grid nesting are conceptually similar and we did not discover any differences (besides the coding differences) that would lead to significantly different model results.

4.4 PLUME-IN-GRID (PiG)

The CAMx and the UAM-V model employ conceptually similar plume-in-grid (PiG) submodels. Major point source emissions are treated as puffs with concentric reactor cells. The puffs entrain ambient air and undergo chemical transformations as they grow and are transported downwind. The puffs are tracked separately until the plume size is commensurate with the grid cell size or layer thickness. The outer concentric reactor cells are shed individually as they grow to the cell thickness. The puffs only interact with the grid cells; they do not interact with other puffs. The CAMx model uses simplified chemistry designed for dealing with major NO_x plumes.

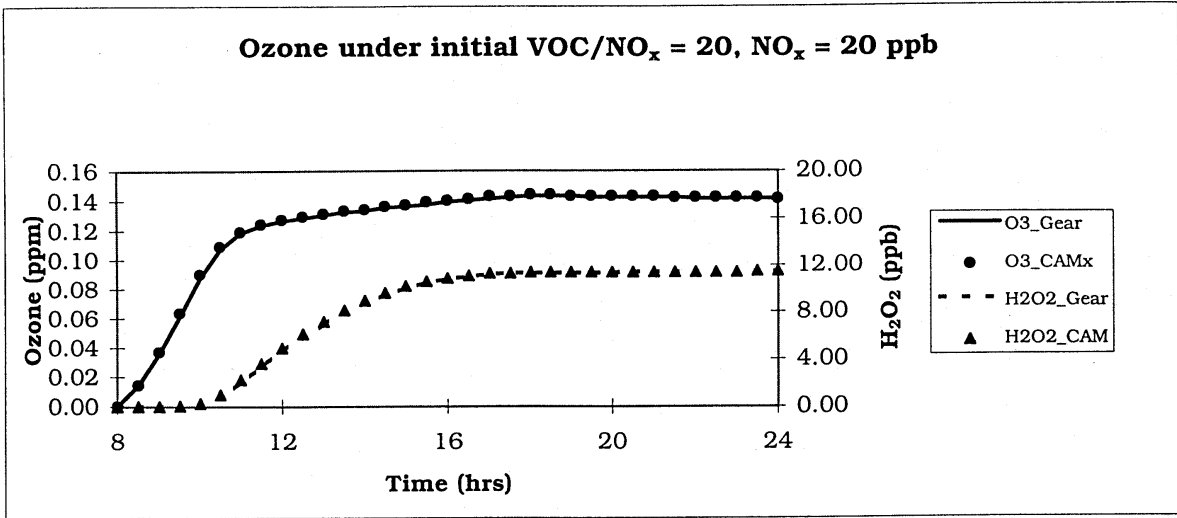


Figure 4-3. Comparison of ozone and H₂O₂ concentrations calculated with the CAMx and LSODE solvers for a daytime initial value problem with an urban VOC mixture, initial VOC/NO_x = 20, and initial NO_x = 20 ppb

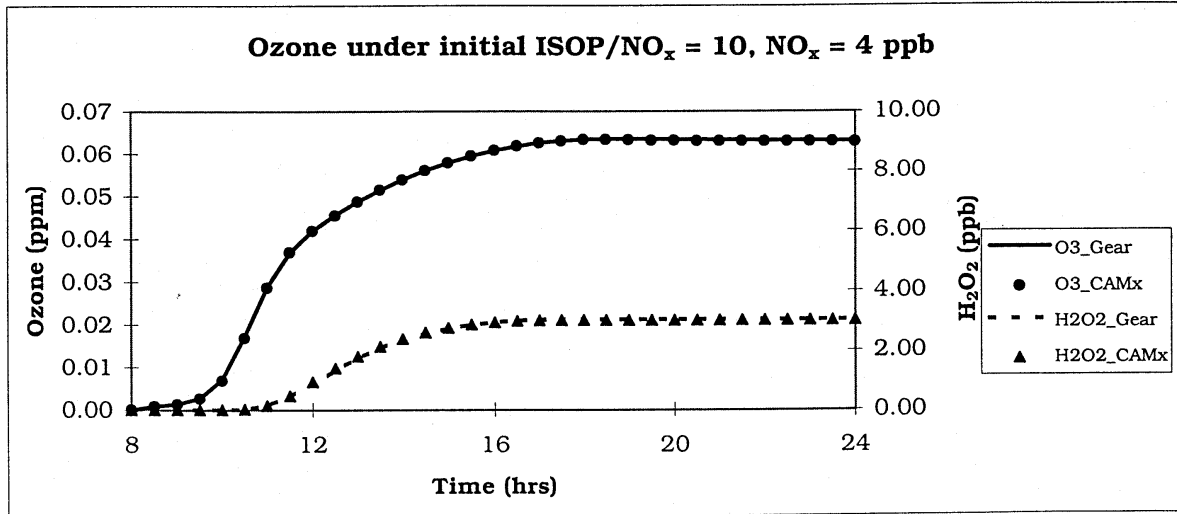


Figure 4-4. Comparison of ozone and H₂O₂ concentrations calculated with the CAMx and LSODE solvers for a daytime initial value problem with initial isoprene/NO_x = 10, and initial NO_x = 4 ppb

The CAMx model includes NO, NO₂, HNO₃, and ozone as state species. The UAM-V usually applies the full chemistry to puffs when NO_x concentrations are below 10 ppm and also has an option for simplified puff chemistry which treats NO, NO₂, HNO₃, ozone, SO₂, and H₂SO₄. The UAM-V has the option to treat the full chemistry in the plumes, but this is rarely used. Minor differences exist in the PiG configurations and the logic for merging the puff mass with the grid cell mass (i.e., terminating puffs). In the OTAG simulations, a 12-hour maximum puff lifetime was used in the CAMx and UAM-V simulations. This length of time is barely adequate for treatment of evening emissions that are injected into stable layers aloft and that must be tracked as puffs until they are entrained into the mixed layer on the following morning. Minor differences in concentrations are expected to result from the differences in PiG treatment in the two models.

4.5 DEPOSITION

The dry deposition modules used by CAMx and UAM-V are both based on the approach of Wesley (1989), yet the implementations differ in several respects. The CAMx implementation uses different parameter values than UAM-V and it uses the surface layer parameterization of Louis (1979) instead of the standard UAM parameterization. The deposition of gases depends strongly on their solubility. The Wesley approach uses the ratio of the solubility of specific gases to the effective solubility SO₂ in calculating their deposition velocities. Because of the S(IV) dissociation reactions, the effective Henry's Law constant for SO₂ is strongly dependent on the pH of the absorbing media (with solubility decreasing with pH). The absorbing surfaces for SO₂, which are mostly leaf tissues, are assumed to be well buffered and the original Wesley inputs assumed a neutral pH. The CAMx implementation used the neutral pH assumption. The UAM-V implementation assumed the absorbing media was acidic, which results in a lower Henry's Law constant for SO₂ than is used in CAMx. The overall effect is that CAMx dry deposition rates generally are higher than those for the UAM-V. We believe the difference in deposition velocities can significantly affect the results over time and, in fact, may explain why the UAM-V simulations have a buildup in ozone towards the end of several OTAG episodes and the CAMx simulations do not.

The CAMx and the UAM-V model have different wet deposition scavenging submodels. These modules are relatively unimportant in ozone modeling and were not examined in this review.

4.6 SUMMARY

The CAMx air quality model has the features one would expect to find in a modern multiscale air quality model. Its formulation is similar in most ways to the UAM-V model. We believe differences in the chemistry numerical solver, the dry deposition algorithm, and the plume-in-grid submodel are likely to cause differences in the predicted concentrations of ozone and other species. Both models use an inaccurate numerical method for advection (Smolarkeiwicz, 1983) that has excessive numerical diffusion (Odman et al., 1996). In

addition, the CAMX code is modern, well structured, and well documented in comparison to the UAM-V code. The differences in code structure may affect the computational speed and convenience of use, but not the model predictions.

5. REFERENCES

- Bott, A (1989): A positive definite advection scheme obtained by nonlinear renormalization of the advective fluxes. *Mon. Wea. Rev.* 117, 1006-1015.
- Chock, D.P., 1991. A comparison of numerical methods for solving the advection equation- III. *Atmos. Environ.*, 25A, 853-871.
- Dabdub, D., Seinfeld, J.H. (1994): Numerical advective schemes used in air quality models - sequential and parallel implementation. *Atmos. Environ.* 28, 3369-3385.
- ENVIRON, 1997. User's Guide to the Comprehensive Air Quality Model with Extensions (CAMx), Version 1.10. ENVIRON International Corporation, Novato, CA.
- Kleinman, L.I. (1991): Seasonal dependence of boundary layer peroxide concentration: the low and high NO_x regimes. *J. Geophys. Res.* 96, 20721-20733.
- Kumar, N. and F.W. Lurmann, 1997. Comparison of the CAMx and UAM-V Model Performance for the July 16-21, 1991 Ozone Episode in the Eastern United States. STI-996303-1713-DR, Sonoma Technology, Inc. report to the Ohio Environmental Protection Agency, Columbus, OH.
- Louis, J.F., 1979. A parametric model of vertical eddy fluxes in the Atmosphere. *Bound. Lay. Meteor.*, 17, 187-202.
- Morris, R.E., Wilson, G.M., Shepard, S.B., and Lee, K., 1997. Ozone Source Apportionment Modeling Using the 1991 OTAG Episode for the Northeast Corridor and Lake Michigan Regions. ENVIRON International Corporation draft report to Cinergy Corporation, Plainfield, IN.
- Odman, M.T., J.G. Wilkinson, L.A. McNair, A.G. Russell, C.L. Ingram, and M.R. Houyoux, 1996. Horizontal Advection Solver Uncertainty in the Urban Airshed Model. Prepared for the California, Air Resources Board, Sacramento, CA.
- SAI, 1995. User's Guide to the Variable-Grid Urban Airshed Model (UAM-V), SYSAPP-95/027. Systems Applications International, San Rafael, CA, April.
- Sillman, S. 1995. The use of NO_y, H₂O₂, and HNO₃ as indicators for ozone-NO_x-hydrocarbon sensitivity in urban locations. *J. of Geophys. Res.*, 100, 14,175-14,188.
- Smolarkiewicz, P.K., 1983. A simple positive definite advection scheme with small implicit diffusion. *Mon. Wea. Rev.*, 111, 479-486.
- Wesely, M.L., 1989. Parameterization of surface resistances to gaseous dry deposition in regional-scale numerical models. *Atmos. Environ.*, 23, 1293-1304.

Yarwood, G., T.E. Stoeckenius, G. Wilson, R.E. Morris, M.A. Yocke, 1996. Development of a Methodology to Assess Geographic and Temporal Ozone Control Strategies for the South Coast Air Basin. ENVIRON International Corporation report to the South Coast Air Quality Management District, Diamond Bar, CA.

Yarwood, G., G. Wilson, R.E. Morris, M.A. Yocke, 1997. User's Guide to the Urban Airshed Model with Ozone Source Apportionment Development. ENVIRON International Corporation report to the South Coast Air Quality Management District, Diamond Bar, CA.